

# O-RAN xApps Conflict Management using Graph Convolutional Networks

Maryam Al Shami, *WIE Member, IEEE*, Jun Yan, *Member, IEEE*, and Emmanuel Thepie Fapi

**Abstract**—Open Radio Access Network (O-RAN) adopts a flexible, open, and virtualized architecture with standardized interfaces, reducing dependency on a single supplier. O-RAN hosts many intelligent applications known as xApps. xApps are applications deployed at the RAN Intelligent Controller (RIC) that leverage advanced AI/ML algorithms to make dynamic decisions for network optimization. Each application operates with distinct optimization objectives and is managed by independent operators while accessing shared network resources. Conflicts in this context occur when a deployed xApp's objective interferes with another xApp, resulting in incompatible actions or decisions that may negatively impact network performance. The lack of a unified mechanism to coordinate and prioritize the actions of different applications can create three types of conflicts (direct, indirect, and implicit). Conflict management in O-RAN refers to the process of identifying and resolving conflicts between network applications. In our paper, we introduce a novel data-driven GCN-based method called GRAPH-based Intelligent xApp Conflict Prediction and Analysis (GRAPHICA) based on Graph Convolutional Network (GCN). It predicts three types of conflicts (direct, indirect, and implicit) and pinpoints the root causes (xApps). GRAPHICA captures the complex and hidden dependencies among the xApps, controlled parameters, and KPIs in O-RAN to predict possible conflicts. Then, it identifies the root causes (xApps) contributing to the predicted conflicts. The proposed method was tested on highly imbalanced synthesized datasets where conflict instances range from 40% to 10%. The model is tested in a setting that simulates real-world scenarios where conflicts are rare to assess its performance. Experimental results demonstrate a high F1-score over 98% for the synthesized datasets with different levels of class imbalance.

**Index Terms**—5G Networks and Beyond, O-RAN, Quality of Service, Conflict Management, xApps, Graph Neural Network, Root Cause Analysis, Predictive Maintenance, Key Performance Indicators.

## I. INTRODUCTION

THE O-RAN represents a paradigm shift in how mobile networks are developed and operated. Traditionally, mobile networks are designed such that each layer of the cellular protocol stack is implemented as a black box with a limited number of vendors. This limits RAN reconfigurability, and coordination among nodes, making it difficult to deploy and integrate equipment from multiple vendors [1]. Motivated by this, O-RAN is introduced to decouple the network's hardware and software components. Thus, promoting interoperability, openness, and flexibility in the design and deployment of RAN components [1].

Service Management and Orchestration (SMO) and Radio Intelligent Controller (RIC) are two important components of the O-RAN architecture. The SMO is responsible for the overall orchestration, management, and automation of the O-RAN [1]. The RIC serves as a platform to deploy applications

that use machine learning models to predict network behavior, detect anomalies, and enhance decision-making capabilities [2]. The intelligent, data-driven control with the RICs is provided through two logical controllers: Non-Real Time RIC (Non-RT RIC) and the Near-RT RIC (Near-RT RIC) [3]. These two RICs provide a platform to host third-party applications that could be powered by machine learning to orchestrate the RAN for specific tasks [4]. They differ in terms of the functions they perform and the timescales over which they operate.

In this context, xApps (eXtended Applications) are software applications designed to run on the Near-RT RIC. These applications are intended to make real-time, fast-paced decisions that immediately impact day-to-day operations and user experiences. xApps play a key role in ensuring Quality of Service (QoS) by providing flexible and dynamic control over various aspects of the network behavior. This includes load balancing [5], interference management [6], and handover optimization [7], [8]. The autonomous operation of xApps managed by different third-party vendors makes them susceptible to conflicts. Each xApp has its own objective and decision-making process. This will introduce new challenges as these applications independently interact with the network environment. The actions of one or more applications could potentially adversely impact the objectives of the others as they share the same network resources or parameters [9]–[11].

Existing solutions leverage AI/ML approaches to address various O-RAN QoS problems. In [12], the authors develop three xApps for Deep Reinforcement Learning (DRL)-based control of RAN slicing, scheduling, and online model training using CoO-RAN. A user-specific O-RAN traffic steering framework for intelligent handovers is unfolded in [13]. The system combines a random ensemble mixture, a conservative Q-learning algorithm, and a convolutional neural network architecture. The paper [14] addresses mobility load balancing and optimization using a random subspace Bayesian additive regression tree and interior point policy optimization for a seamless user experience. In [15], the authors introduce a DRL-based radio resource management solution for RAN slicing with guaranteed service-level agreement.

Other studies seek to detect or predict the occurrences of conflicts in O-RAN. In [16], a team deep Q-learning algorithm for resource allocation is disclosed to mitigate xApps conflicts in O-RAN. In [17], a bargaining game-theoretic approach is introduced along with a standardized Conflict Mitigation System (CMS) and independent controllers. This work is further improved in [18]. The authors use a cooperative game theory to optimize the conflicting parameters while maximizing the

number of xApps that meet QoS requirements. In [19], a Deep Q-Network and a multi-headed multilayer perceptron network model are presented. The method distills knowledge from multiple xApps to train a single model retaining the capabilities of previous xApps.

Other works address the xApps conflict management using graph-based approaches. The authors in [20] propose a method to detect, characterize, and mitigate conflicts among applications in O-RAN. Accordingly, they combine hierarchical graphs with statistical knowledge of applications to find dependencies between control parameters and Key Performance Measurements. In [21], the paper suggests using GraphSAGE for reconstructing and labeling conflict graphs in O-RAN. It captures the hidden dependencies between xApps, parameters, and KPIs. Then, graph labeling is performed to identify the different types of conflicts based on well-defined, graph-based definitions.

Understanding the complex and intricate dependencies between the xApps, the controlled parameters, and the KPIs is imperative to address the xApp conflict RCA. It allows us to predict the different types of conflicts in real time and derive the contributing root causes (xApps) for proactive maintenance. In the previously mentioned non-graph-based approaches, there is still a substantial limitation in their capacity to effectively capture and model dependencies within complex data structures. The proposed method in [21] leverages GraphSAGE to effectively capture the dependencies within the data. However, it still falls short of fully accounting for the imbalanced nature of the datasets in practical life scenarios, as these conflicts are rare. Addressing this limitation is crucial for enhancing the robustness and generalizability of the proposed approach in real-world applications. Accordingly, we propose GRAPHICA, a GCN-based method that is capable of handling highly imbalanced datasets with up to 10% conflicts. It predicts the xApps conflicts (direct, indirect, and implicit) and identifies their root causes (xApps) for future mitigation strategies.

Our technical contributions are as follows:

- We propose a 5G O-RAN xApps conflict prediction with a root cause analysis method using Graph Convolutional Networks (GCNs). This allows us to capture the complex and hidden dependencies between the xApps, parameters, and KPIs in the network to predict xApps conflicts (direct, indirect, and implicit).
- We leverage a binary state-based GCN structure to map and explain the complex relationships. This ensures the generalizability of the proposed solution, which can be extended to other networks. This structure along with the predictions are the key inputs for the root cause analysis.
- We use the focal loss function in the model training. This allows the model to handle highly imbalanced datasets. The model maintains an F1 score greater than 98% for the synthesized datasets with different levels of class imbalance.

The remainder of this paper is structured as follows. Section II presents the problem formulation, clearly defining the research question and outlining the scope and objectives of the study. Section III describes the proposed system model.

Section IV details the evaluation metrics, the experimental setup, and the interpretation of the results. Section V discusses the results derived from the analysis. Section VI concludes this paper.

## II. PRELIMINARIES

Conflict management is a crucial aspect of O-RAN, ensuring different applications operate harmoniously within the network. The conflicts can be categorized into three types: Direct, indirect, and implicit conflict [20], [22], [23]. Fig. 1 illustrates the various types of conflicts in the network.

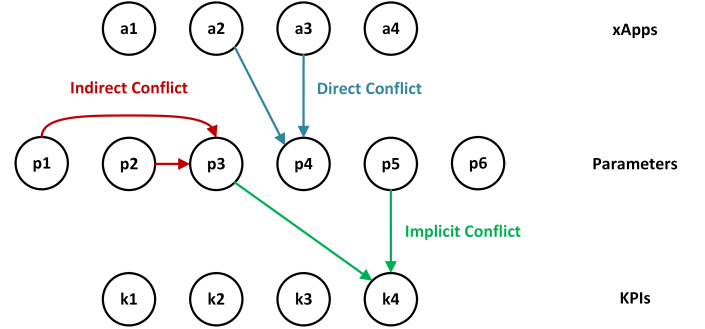


Fig. 1. Examples of xApps conflicts.

Direct conflicts arise when multiple applications attempt to modify or request different settings for the same network parameter simultaneously. These conflicts are easily noticeable and can result in immediate service degradation, unstable performance, or even network failures if not promptly addressed. For example, two xApps might attempt to adjust the transmission power of the same cell simultaneously. In particular, one xApp seeks to increase power for better coverage, while the other aims to reduce it to minimize interference with neighboring cells.

Indirect conflicts are not immediately visible, but the interdependencies between the parameters and resources involved can be observed. These conflicts occur when multiple applications modify a set of parameters that directly affect the values of other parameters. They are subtler than direct conflicts and may result in unintended negative effects. For instance, one xApp may optimize load balancing by redistributing traffic across various cells, while another xApp is adjusting handover parameters to enhance mobility performance. Although these actions are independent, the resulting traffic shifts could disrupt the handover process or increase congestion in certain cells, leading to a degraded user experience.

Implicit conflicts transpire when multiple xApps make control decisions that target different optimization objectives, which interfere with one another. These conflicts are not directly observable. They depend on intrinsic relationships between control parameters and observable Key Performance Indicators (KPIs). They are more abstract and arise from differences in how xApps interpret the network's requirements. For instance, one xApp might prioritize energy efficiency by reducing transmission power across several cells to lower consumption. Meanwhile, another xApp seeks to increase

power in certain areas to enhance coverage. The conflicting goals, energy efficiency versus coverage, could lead to poor service quality in some areas of the network or result in inefficient power usage.

Grasping the distinctions between these conflicts in O-RAN is crucial for developing resilient, automated networks. The network must be capable of efficiently handling various optimization goals such as Quality of Service (QoS), coverage, and energy efficiency. Effective conflict management is necessary as a tailored resolution approach to maintain optimal network performance while achieving specific objectives. This process involves detecting, predicting, resolving, and preventing conflicts between the decisions and actions of xApps.

Dealing with xApps in an O-RAN environment brings many critical challenges that need to be addressed. This involves ensuring that multiple xApps can operate simultaneously and complement each other, leading to a well-optimized network. Specifically, there is a lack of coordination and standardization among the various components responsible for RAN control decisions. Moreover, in large, complex, and hierarchical networks, it is impossible to be able to update the conflict management configuration manually. In addition, as multiple conflicting objectives could co-exist, finding a single optimal solution that optimizes all the objectives may not be feasible. This will make it difficult to identify the conflicts along with their root causes to address them with appropriate mitigation strategies [9], [11].

### III. PROPOSED METHOD

We now introduce our proposed solution conflict model. The proposed framework is depicted in Fig. 2. The Near-RT RIC serves as a key point of collection for the xApps states, the values of the controlled parameters data, and KPI metrics. These data are collected leveraging the subscription manager (SM), which is a part of the Near-RT RIC. SM is responsible for handling the xApps subscriptions. It manages which xApps are subscribed to specific events, KPIs, or data sources from the RAN. Additionally, it tracks the active subscriptions and ensures that xApps receive the data they need. To retrieve the list of the activated xApps, the parameters, and the KPIs, we should interact with the RIC platform via the RIC API.

A database is required to store the collected data from the SM in the Near-RT RIC using the messaging infrastructure. Then, the proposed system retrieves the collected data from the database for further processing using a shared data layer. Our proposed solution requires the implementation of a component that converts the collected data into a binary-state dataset, as depicted in Fig. 4. In particular, the state of an activated xApp is presented by “1”, and a deactivated xApp is represented by “0”. Similarly, if the value of a parameter or a KPI is changed from its previous timestamp value, the state is set to “1”, otherwise, the state is set to “0”.

The proposed solution executes three major tasks, namely Graph Structure Creator (GSC), Graph Anomaly Predictor (GAP), and Root Cause Analyst (RCA). Fig. 3 illustrates the chronological sequence of events, highlighting the progression from system monitoring to conflict occurrence. The predictive

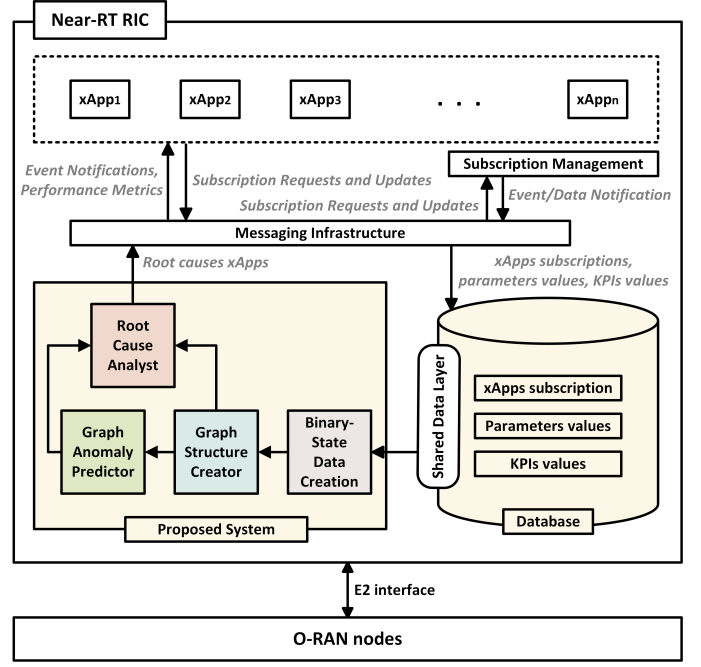


Fig. 2. The proposed framework.

model utilizes real-time data and a GCN-based model to identify key triggers based on dynamic variables in the network and forecast the likelihood of a conflict occurrence. Specifically, at time  $t_0$ , the proposed system initiates the monitoring process and undergoes a collection for the state dynamic behavior, including the xApps subscription, operational parameters, and KPIs values. At  $t_1$ , an alert is raised based on the observed patterns if there is a likelihood of a deviation or anomaly in the system's behavior and the possible root causes (xApps) are identified to trigger a need for immediate attention and intervention. If the alert is raised in time before the conflict occurs at  $t_2$ , we can avoid a later KPI degradation at  $t_3$ . In the remainder of this section, we will describe each module in the proposed method, outlining the corresponding steps and functionality.

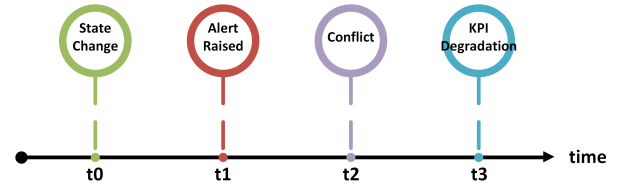


Fig. 3. The chronological sequence of events for conflicts prediction.

#### A. Data Curation and Conflicts Modeling

We will thoroughly explain the dataset generation and the modeling of the three types of conflict steps. Let  $\mathcal{A}$  be the set of O-RAN xApps deployed on the Near-RT RIC. Let  $\mathcal{P}$  be the set of parameters that are controlled by applications in  $\mathcal{A}$ , and  $\mathcal{K}$  be the set of observable KPIs.

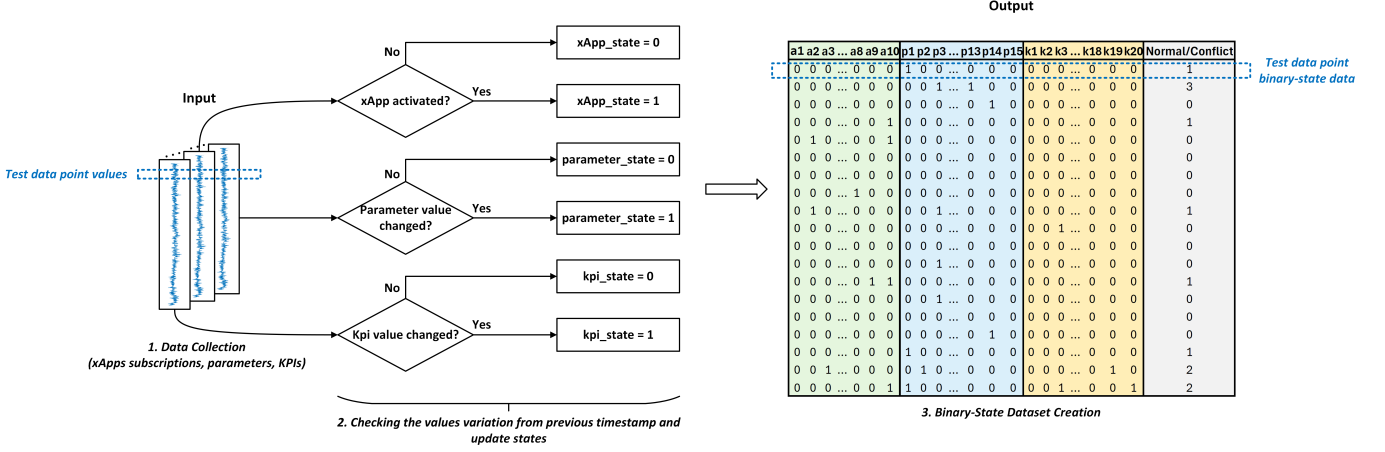


Fig. 4. The binary-state data creation module steps.

For each application  $a \in \mathcal{A}$  and parameter  $p \in \mathcal{P}$ , we define a state indicator  $i_{p,a} \in \{0,1\}$  such that  $i_{p,a} = 1$  if application  $a$  controls parameter  $p$ , and  $i_{p,a} = 0$  otherwise. For each KPI  $k \in \mathcal{K}$  and parameter  $p \in \mathcal{P}$ , we define another state indicator  $j_{k,p} \in \{0,1\}$  such that  $j_{k,p} = 1$  if parameter  $p$  modifies the value of KPI  $k$ , and  $j_{k,p} = 0$  otherwise. For each parameter  $p \in \mathcal{P}$ , we create a copy of the set  $\mathcal{P}$  called  $\mathcal{P}'$  and a random parameter  $p' \in \mathcal{P}'$  is chosen such that this parameter is removed from the set  $\mathcal{P}$ . Then, we define another state indicator  $l_{p,p'} \in \{0,1\}$  such that  $l_{p,p'} = 1$  if parameter  $p$  modifies the value of parameter  $p'$ , and  $l_{p,p'} = 0$  otherwise.

Conflict modeling is performed by randomly selecting elements from each set and mapping them to the elements in the other set without any predetermined pattern or order. This is achieved by shuffling the sets and randomly assigning the elements in the shuffled set to those in the other set. The randomness of the assignment ensures that there is no bias or regularity in the mapping. Each variable has an equal chance of being paired with any other variable from the second set to introduce diversity in the assignments.

Accordingly, five binary-state datasets are generated. Each dataset  $D$  contains a target label column that classifies each data point into one of four distinct classes (0: normal, 1: direct conflict, 2: implicit conflict, and 3: indirect conflict). The first dataset is balanced, and the classes are evenly distributed. The remaining four datasets are generated with different conflict proportions ranging from 40% to 10%. The core idea behind this diversity is to test our model on generated datasets close to real-world scenarios where conflicts are rare.

### B. Graph Structure Creator (GSC)

The GSC module is responsible for creating graph-structured data from the binary-state dataset comprising the collected data from the Near-RT RIC (see Fig. 5). The GSC ingests the binary-state dataset and the number of xApps, parameters, and KPIs as input and convert them into graph-structured data for further processes using three subgraphs:  $G^{\text{PA}}$ ,  $G^{\text{KP}}$ , and  $G^{\text{P'P}}$ .

The subgraph  $G^{\text{PA}} = (V^{\text{PA}}, E^{\text{PA}})$  represents the relationships between the applications and the control parameters. Nodes of  $G^{\text{PA}}$  are both the applications and the control parameters, i.e.,  $V^{\text{PA}} = \mathcal{P} \cup \mathcal{A}$ , and edges  $E^{\text{PA}}$  represent whether or not an application is controlling a parameter  $p \in \mathcal{P}$ . Any 2-tuple  $(p, a) \in \mathcal{P} \times \mathcal{A}$  is an edge of  $G^{\text{PA}}$ , i.e.,  $(p, a) \in E^{\text{PA}}$  if and only if parameter  $p$  is directly controlled by an application  $a$ . This will cause a direct conflict.

The subgraph  $G^{\text{KP}} = (V^{\text{KP}}, E^{\text{KP}})$  represents the relationships between the control parameters and the KPIs. Nodes of  $G^{\text{KP}}$  are both the parameters and the KPIs, i.e.,  $V^{\text{KP}} = \mathcal{K} \cup \mathcal{P}$ , and edges  $E^{\text{KP}}$  represent whether or not a parameter is modifying the value of a KPI  $p \in \mathcal{P}$ . Any 2-tuple  $(k, p) \in \mathcal{K} \times \mathcal{P}$  is an edge of  $G^{\text{KP}}$ , i.e.,  $(k, p) \in E^{\text{KP}}$  if and only if KPI  $k$  is directly affected by a parameter  $p$ . This will cause an indirect conflict.

The subgraph  $G^{\text{P'P}} = (V^{\text{P'P}}, E^{\text{P'P}})$  represents the relationships between the control parameters themselves. Nodes of  $G^{\text{P'P}}$  are both the parameters in the sets  $\mathcal{P}'$  and  $\mathcal{P}$ , i.e.,  $V^{\text{P'P}} = \mathcal{P}' \cup \mathcal{P}$ , and edges  $E^{\text{P'P}}$  represent whether or not a parameter  $p \in \mathcal{P}$  is modifying the value of another parameter  $p' \in \mathcal{P}'$ . Any 2-tuple  $(p', p) \in \mathcal{P}' \times \mathcal{P}$  is an edge of  $G^{\text{P'P}}$ , i.e.,  $(p', p) \in E^{\text{P'P}}$  if and only if a parameter  $p'$  is directly affected by a parameter  $p$ . This will cause an implicit conflict.

To construct the graph  $G^{\text{PA}}$ , the GSC iterates over the applications and the parameters nodes and stores their corresponding state values. Subsequently, the resultant graph nodes are xApps and the parameters. The edges represent the nodes having a state "1" concurrently. The edges reflect the nodes that are affecting each other at the same time. This leads to direct conflicts.

Similarly, for  $G^{\text{KP}}$ , the GSC iterates over the parameters and the KPIs nodes and stores their corresponding state values. The output graph nodes are the parameters and the KPIs. The edges indicate the parameters and KPIs whose values change simultaneously by with a state "1", resulting in implicit conflicts.

Lastly, for  $G^{\text{P'P}}$ , the GSC iterates over the parameters and checks their state values. The nodes of the graphs are

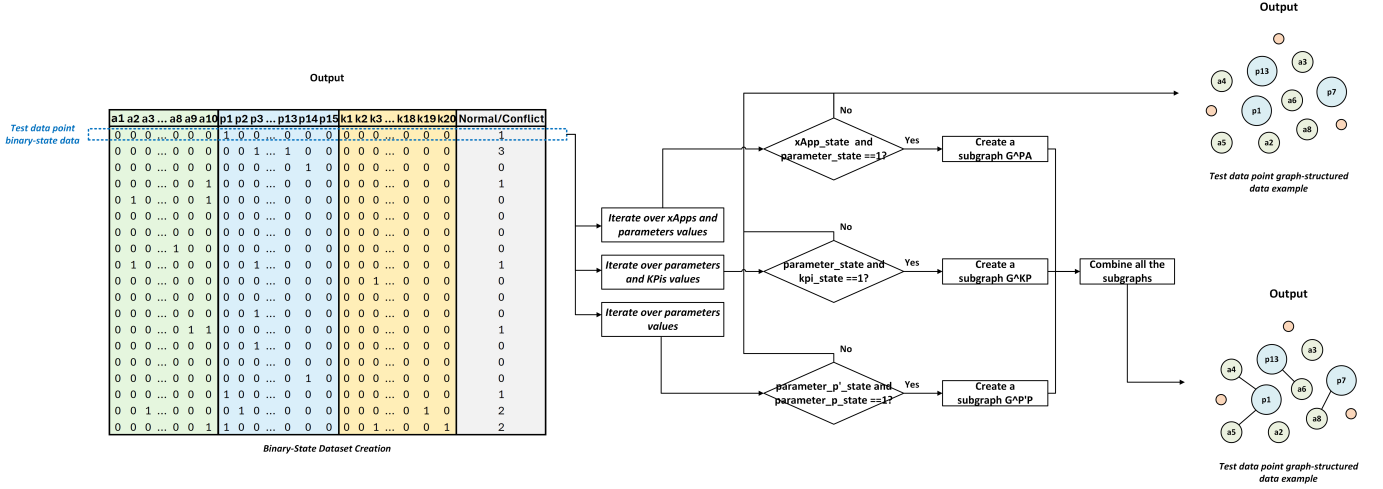


Fig. 5. The graph structure creator (GSC) module.

the parameters, and the edges refer to the links among the parameters that have a state of “1”. This means the parameters are impacting each other’s behavior. This produces indirect conflicts.

During the construction of the three subgraphs, unique node features and edge attributes are assigned to the nodes and their edges, contributing to the same type of conflict. GCN uses node features as the starting point to update the node embeddings (representations) through multiple layers of convolutions. These embeddings are refined iteratively as the model propagates information across neighboring nodes. Including edge attributes in the graph convolution process allows the model to learn a more nuanced understanding of node interactions. When performing convolution, edge attributes help the GCN understand the nature of the relationship between nodes.

### C. Graph Anomaly Predictor (GAP)

The GAP module is responsible for predicting whether the instance is normal or whether we have a conflict (see Fig. 6). The output of GAP will be one of four labels (0: normal, 1: direct conflict, 2: implicit conflict, and 3: indirect conflict). The fully constructed graph structure from the GSC module is fed to the GAP module. It consists of a Graph Convolutional Network (GCN). GCN learns node-level representations from the graph-structured data, which are then aggregated via a global mean pooling into a graph-level representation for final classification. Then, a fully connected neural network (NN) layer is used to learn the final transformation from the graph’s representation to the output classes.

To address the imbalances in the datasets, the classifier is enhanced by a focal loss function [24]. It improves the standard cross-entropy loss by adding two key parameters, alpha and gamma. This function adjusts the loss contribution of easy and hard examples. It focuses more on hard-to-classify examples that are misclassified by the model. In parallel, it down-weights the loss associated with easy-to-classify examples.  $\alpha_c$  adjusts for class imbalance by balancing the weight between

different classes.  $\gamma$  focuses the model on harder examples by reducing the loss for easy, well-classified examples. This helps to prevent the model from being overwhelmed by the majority class in imbalanced datasets and gives more attention to challenging instances. We compute  $\alpha_c$  using inverse class weights by calculating the inverse frequency of each class in the dataset. On the other hand,  $\gamma$  is manually tuned for model optimization. The focal loss function for multi-class classification is given by:

$$\mathcal{L}_{\text{focal}} = - \sum_{c=1}^C \alpha_c (1 - p_{t_c})^\gamma \log(p_{t_c}) \quad (1)$$

where:

- $C$  is the number of classes.
- $p_{t_c}$  is the predicted probability for the true class  $c$ .
- $\alpha_c$  is the weighting factor for class  $c$ , which can help address class imbalance.
- $\gamma$  is the focusing parameter, which down-weights the loss for well-classified examples.

For each sample, this loss function is computed by summing the individual losses for each class, where only the true class  $c$  contributes to the loss.  $p_{t_c}$  is defined as the predicted probability for the true class.

The model consists of a two-layer GCN. GCN is a type of GNN designed specifically to operate on graph-structured data. It operates by propagating node features through the graph, aggregating information from a node’s neighbors, and learning a new representation for each node. The process is typically iterative (layer-wise), with each layer performing a graph convolution operation.

After passing through two layers of graph convolution, the final node representations are passed through a fully connected layer to perform graph classification. A mean pooling mechanism is applied to the node features. It aggregates information into a graph-level representation before making the final classification.

Instead of processing the entire graph at once, mini-batch processing is executed. This involves processing smaller sub-



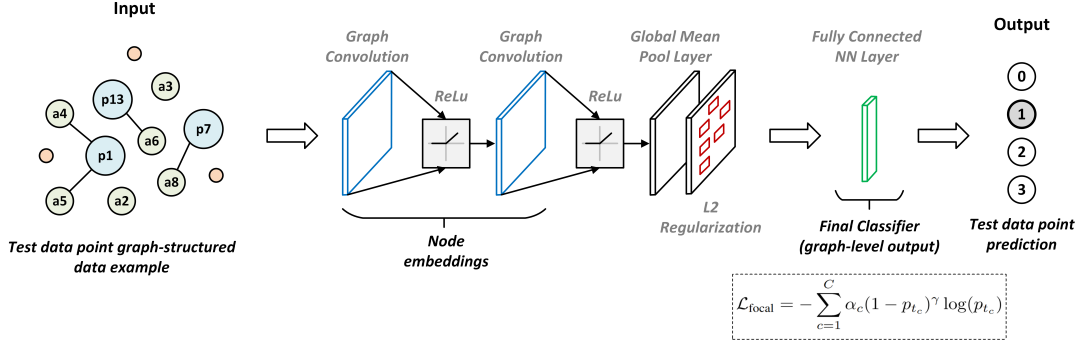


Fig. 6. The graph anomaly predictor module.

graphs simultaneously, which helps reduce memory usage and computational time. Furthermore, a stratified K-Fold is implemented to ensure that each fold in the cross-validation process has a similar distribution of classes as the entire dataset during training and validation. This is particularly useful since real-world traffic is highly imbalanced. Early stopping is implemented in our model which is a method used to prevent overfitting by monitoring the validation loss during training, and halting the training process if the model's performance on the validation set does not improve for a specified number of epochs. The delta ensures that only considerable improvements in validation loss are evaluated as indicators of progress, preventing early stopping from being triggered by negligible changes.

The L2 regularization is implemented to mitigate overfitting. The L2 regularization adds a penalty to the loss function that prevents the model from giving too much weight to any single feature. It achieves this by squaring the model's weights and adding the result to the loss, causing the model to prefer lower weight values. The equation for L2 regularization is given by:

$$\mathcal{L}_{L2} = \lambda \sum_{i=1}^n w_i^2 \quad (2)$$

where  $\lambda$  is the regularization parameter controlling the strength of the regularization,  $w_i$  is the weight for the  $i$ -th feature in the model, and  $n$  is the total number of weights in the model.

#### D. Root Cause Analyst (RCA)

The RCA module is responsible for explaining the GAP module predictions by providing the root causes (xApps) contributing to the predicted conflicts (see Fig. 7). The predictions from GAP and the whole constructed graph structure obtained from GSC are passed to the RCA module. The output is a subset of the graph of the predicted conflicts.

The subset of the graph corresponding to each prediction is further analyzed. RCA checks the source node with more than one incoming edge, as shown in Fig. 1. This means that the behavior of this node is being altered by more than one node. Then, RCA extracts the connected destination nodes as the root causes contributing to the predicted conflict.

Addressing the root causes proactively improves long-term performance and system stability. A proactive approach relies

on a deep understanding of the factors contributing to a problem. By analyzing data to uncover the root causes of service degradation in the network, mobile operators can make informed decisions to avoid reactive responses that are often incomplete or insufficient.

## IV. EXPERIMENTS AND RESULTS

This section presents the experimental setup and performance of the proposed solution. The experimental setup outlines the environment, tools, and methodologies employed to assess the effectiveness of GRAPHICA, while the results provide a comprehensive interpretation and analysis of its performance.

#### A. Experimental Setup

To evaluate the performance of our method, we use precision (Prec), recall (Rec) and F1-Score (F1) over the test dataset and its ground truth values:  $F1 = \frac{2 \times \text{Prec} \times \text{Rec}}{\text{Prec} + \text{Rec}}$ , where  $\text{Prec} = \frac{TP}{TP+FP}$  and  $\text{Rec} = \frac{TP}{TP+FN}$ . TP, TN, FP, and FN represent true positives, true negatives, false positives, and false negatives, respectively. Our generated datasets are highly imbalanced, which justifies the choice of these metrics that are suitable for imbalanced data.

We simulated and tested our model on an NVIDIA DGX station Intel(R) Xeon(R) CPU ES-2698 v4 @2.20GHz, 20core/40ht with 256GB of memory. The model is trained using the Adam optimizer with a learning rate 0.01, ReLU activation function, and a weight decay 1e-4. The training process utilizes a batch size of 128, employing 5-fold cross-validation over 2,000 epochs. A two-layer GCN model operates on the graph's node features. It performs graph convolutions and aggregates information from the graph structure. Global mean pooling [25] is applied to return batch-wise graph-level-outputs by averaging node features across the node dimension.

#### B. Experiment Results

We conducted a parametric study provided by Table I to demonstrate the model's performance under different values of  $\gamma$ , where the imbalance may have a strong impact on the model's effectiveness.

For the balanced dataset,  $\gamma$  is set to zero in the focal loss function as the classes are equally distributed. All the classes

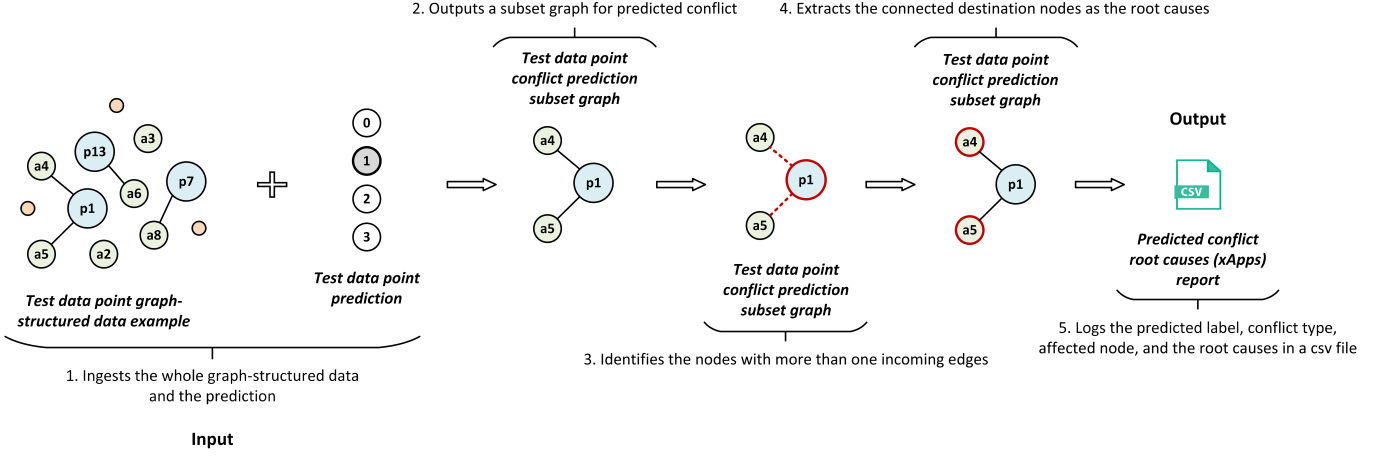


Fig. 7. The root cause analyst (RCA) module.

contribute similarly to the loss function, and the model is less likely to be biased toward the majority class. The model demonstrates remarkable performance on the balanced dataset, achieving high precision, recall, and F1 of 0.9829, 0.9818, and 0.9817, respectively.

We evaluated the proposed model for more  $\gamma$  values, spanning from 0.0 to 4.0, and computed the average performance across ten experiments. This analysis was performed on the imbalanced datasets under investigation, as shown in Table I. As the value of  $\gamma$  increases, the performance metrics improve for all the datasets. The best performance is attained when  $\gamma$  reaches 1.5 for the 40% conflict dataset and 2.0 for the 30%, 20%, and 10% conflict datasets, respectively. At these values, the model achieves an F1-score of 0.9930, 0.9946, 0.9908, and 0.9954, respectively. Afterward, the performance metrics begin to decrease. This reduction in performance is expected, as excessively high values of  $\gamma$  cause the model to overly focus on misclassified examples, potentially leading to overfitting. This, in turn, reduces the model's ability to generalize to easier examples, resulting in a decrease in overall performance.

The variation of  $\gamma$  significantly influences the model's performance. As  $\gamma$  increases, the model emphasizes hard-to-classify examples during the training phase, thereby enhancing recall by improving its ability to identify difficult or underrepresented cases. However, this focus on challenging examples can reduce precision, as the model may misclassify some simpler instances. Conversely, when  $\gamma$  is set to a lower value, the model treats all examples with equal importance during training, resulting in a more balanced performance. However, this may limit the model's capacity to focus on difficult cases adequately. Therefore, selecting the optimal  $\gamma$  value is crucial for achieving a balance between precision and recall, ensuring the model performs effectively without overfocusing on any particular type of conflict. Overall, as shown in Table I, the model exhibits consistent precision, recall, and F1 across different test datasets with varying levels of imbalance.

For further illustration, the training and validation losses across epochs for 10 experiments for the 10% conflict dataset

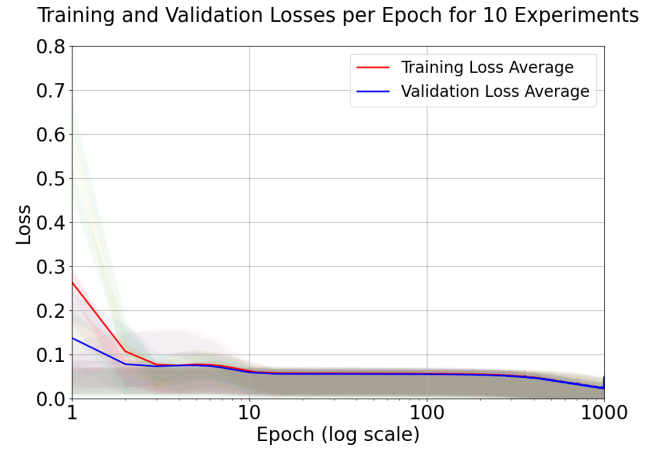


Fig. 8. Training and validation losses per epoch on the 10% conflict dataset.

( $\gamma = 2.0$ ) are shown in Fig. 8, represented as shaded regions to show variability, with bold lines indicating the average training and validation trends. The losses decrease throughout training. This indicates that the model is effectively learning from the data over time. Initially, both losses were high. This reflects the model's early stage of learning, where it struggles to fit the data. As the training progresses, the loss decreases, indicating that the model is gradually learning to make better predictions on the training data. Thus, the model improves its ability to fit the training data and gradually minimizes the error between its predictions and the actual values. Similarly, the validation loss decreases, suggesting that the model is generalizing well and not overfitting to the training set. Both losses decrease at a similar rate and converge to a low value of less than 0.05. The decreasing losses typically point to a well-optimized model, learning meaningful patterns and avoiding excessive complexity or bias.

The confusion matrix (CM) of the proposed method testing on the 10% conflict dataset ( $\gamma = 2.0$ ) is shown in Fig. 9. The test set consists of 114 data points. Among these, 97 are predicted as normal, 6 as direct conflicts, 3 as implicit

TABLE I  
AVERAGE PERFORMANCE OF GCN IN DIFFERENT SETUPS

Test Datasets		Performance								
		$\gamma=0.0$	$\gamma=0.5$	$\gamma=1.0$	$\gamma=1.5$	$\gamma=2.0$	$\gamma=2.5$	$\gamma=3.0$	$\gamma=3.5$	$\gamma=4.0$
40% conflict	Prec	0.9849	0.9879	0.9900	0.9937	0.9923	0.9930	0.9923	0.9889	0.9892
	Rec	0.9809	0.9861	0.9890	0.9931	0.9913	0.9919	0.9913	0.9873	0.9867
	F1	0.9802	0.9859	0.9889	<b>0.9930</b>	0.9914	0.9918	0.9912	0.9871	0.9867
30% conflict	Prec	0.9837	0.9884	0.9897	0.9929	0.9951	0.9915	0.9904	0.9906	0.9886
	Rec	0.9804	0.9865	0.9878	0.9919	0.9946	0.9899	0.9878	0.9892	0.9872
	F1	0.9795	0.9864	0.9876	0.9919	<b>0.9946</b>	0.9898	0.9875	0.9888	0.9869
20% conflict	Prec	0.9648	0.9633	0.9792	0.9848	0.9939	0.9854	0.9834	0.9885	0.9867
	Rec	0.9633	0.9641	0.9828	0.9836	0.9914	0.9820	0.9836	0.9828	0.9820
	F1	0.9568	0.9586	0.9797	0.9824	<b>0.9908</b>	0.9818	0.9820	0.9814	0.9807
10% conflict	Prec	0.9721	0.9760	0.9913	0.9954	0.9960	0.9871	0.9894	0.9766	0.9605
	Rec	0.9816	0.9842	0.9798	0.9947	0.9956	0.9860	0.9895	0.9781	0.9702
	F1	0.9757	0.9792	0.9798	0.9945	<b>0.9954</b>	0.9854	0.9878	0.9735	0.9630

TABLE II  
AN EXAMPLE OF CONFLICT REPORT BY THE RCA (10% CONFLICT)

Predicted Label	Conflict Type	Affected Node	Root Causes Nodes	Root Causes xApps
1	Direct	p12	a1, a3	a1, a3
3	Indirect	p8	p1, p3	a1, a3
1	Direct	p2	a4, a6	a4, a6
2	Implicit	k10	p1, p9	a1, a9
1	Direct	p10	a2, a5, a8	a2, a5, a8
3	Indirect	p13	p7, p9, p10	a7, a9, a10
2	Implicit	k5	p4, p2	a4, a2

conflicts, and 7 as indirect conflicts. In this highly imbalanced scenario, where the normal cases significantly outnumber the conflicts, only 1 implicit conflict was misclassified as an indirect one. This indicates that the model can generalize well in imbalanced data.

The conflict RCA report for the 10% conflict test dataset ( $\gamma = 2.0$ ) is illustrated in Table II. The normal data points in the table are filtered to emphasize the predicted conflicts. The report elucidates the predicted label, the type of the conflict, the affected node, and the root causes (nodes and xApps). The affected node is the one whose behavior is altered by one or more nodes. The root causes nodes are the nodes that are concurrently modifying the same node, and the root causes (xApps) are the applications contributing to the predicted conflict.

As an example, the first line of the report indicates the occurrence of a direct conflict (predicted label = 1). The value of the parameter p12 is influenced by the xApps a1 and a3. Consequently, the root causes of this direct conflict are identified as the xApps a1 and a3. The last line of the report reveals an implicit conflict, with the predicted label being 2. In particular, the value of kpi k5 is affected by two parameters (p4 and p2), which are controlled by the xApps a4 and a2, respectively. Therefore, the root causes of this conflict are the xApps a4 and a2.

## V. DISCUSSIONS

While the demonstrated performance is outstanding on the curated datasets, to the best of our knowledge, there

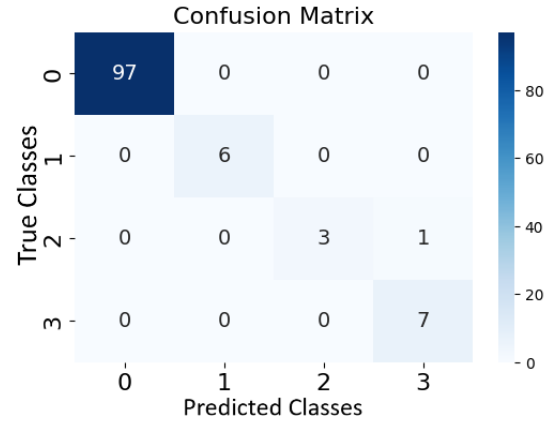


Fig. 9. Confusion matrix on the 10% conflict test dataset.

is a lack of publicly available datasets or benchmarks for comparing the performance against other approaches to xApp conflict analysis. In [17], [18], [21], the proposed methods are tested on simulated synthetic data based on the Gaussian distribution function to generate KPIs for xApps. In [20] and [19], simulations are developed using network emulators such as the Colosseum wireless network emulator and “mobile-env” wireless communication environment in the Gymnasium framework, respectively. A key extension of the work is to enrich the scenarios and release, where applicable, a benchmark with open data from real or realistic O-RAN in 5G/beyond 5G. This would allow further validation and comparisons of different methods in practical scenarios.

Our results are still sufficiently good without benchmarking against others because the missed conflicts, although mostly implicit, are generally mild. The more severe conflicts are effectively flagged promptly. Our approach is particularly effective in practical applications, as it efficiently enables early prediction of rare conflict scenarios up to 10%, providing ample time for preventive measures to be put in place.

Compared to other works such as the one presented in [21], which claims an exceptionally high performance of 100%, our method is not inherently underperforming. Instead, it avoids reliance on potentially unrealistic benchmarks. Existing



methods [17], [18], [21] are heavily distribution-dependent, often predicated on the assumption that the underlying data follows a Gaussian distribution, which is used to assign values to KPIs. However, in practical, real-world applications, KPIs frequently exhibit more complex behaviors and may not conform to Gaussian distributions. Our approach addresses this limitation by being distribution-independent, where KPIs are assigned binary state values based on their dynamic behavior. This design enables our methodology to generalize effectively across diverse KPI contexts without being constrained to specific distributions. Consequently, it can be argued that our method offers a superior level of adaptability and robustness for applications where distribution assumptions may not hold.

## VI. CONCLUSION

In this work, we proposed a novel data-driven GCN-based method called GRAPHICA for xApps conflict management and RCA in O-RAN. Our approach takes a binary-state dataset as input and constructs graph-structured data. The binary state dataset encapsulates the dynamic variations in the values of the xApps subscriptions, controllable parameters, and KPIs within the network. Our Proposal leverages focal loss function to predict three types of conflicts (direct, indirect, and implicit). The RCA module then processes the learned graph structure and the predictions to determine the xApps being the source of the predicted conflict. The model demonstrates high performance on highly imbalanced datasets. With a presence of conflicts ranging from 40% to 10%, the proposed model architecture achieves an F1 score greater than 98% on various evaluation metrics for all the synthesized datasets. Future work will focus on developing predictive maintenance with mitigation strategies based on the retrieved root causes to prevent performance degradation and reduce xApp conflicts across multi-vendor environments. Additionally, we plan to deploy and test the model in a real-life environment to further enhance its performance and applicability.

## REFERENCES

- [1] M. Polese, L. Bonati, S. D'Oro, S. Basagni, and T. Melodia, "Understanding o-ran: Architecture, interfaces, algorithms, security, and research challenges," *IEEE Communications Surveys & Tutorials*, vol. 25, no. 2, pp. 1376–1411, 2023.
- [2] B. Balasubramanian, E. S. Daniels, M. Hiltunen, R. Jana, K. Joshi, R. Sivaraj, T. X. Tran, and C. Wang, "Ric: A ran intelligent controller platform for ai-enabled cellular networks," *IEEE Internet Computing*, vol. 25, no. 2, pp. 7–17, 2021.
- [3] L. Bonati, S. D'Oro, M. Polese, S. Basagni, and T. Melodia, "Intelligence and learning in o-ran for data-driven nextg cellular networks," *IEEE Communications Magazine*, vol. 59, no. 10, pp. 21–27, 2021.
- [4] M. Wani, M. Kretschmer, B. Schröder, A. Grebe, and M. Rademacher, "Open ran: A concise overview," *IEEE Open Journal of the Communications Society*, vol. 6, pp. 13–28, 2025.
- [5] R. Ntassah, G. M. Dell'Aera, and F. Granelli, "xapp for traffic steering and load balancing in the o-ran architecture," in *ICC 2023 - IEEE International Conference on Communications*, 2023, pp. 5259–5264.
- [6] D. Anand, M. A. Togou, and G.-M. Muntean, "Enhancing qoe diversity in hetnets through interference mitigation with ml-based xapp in a 5g o-ran architecture," in *ICC 2024 - IEEE International Conference on Communications*, 2024, pp. 5473–5478.
- [7] B. H. Prananto, Iskandar, Hendrawan, and A. Kurniawan, "Lstm neural network algorithm for handover improvement in a non-ideal network using o-ran near-rt ric," *IEICE Transactions on Communications*, vol. E107-B, no. 6, pp. 458–469, 2024.
- [8] P. Cumino, J. Baranda, M. Luis, D. Rosario, E. Cerqueira, J. Mangues, and S. Sargento, "Enhancing mobile network performance through oran-integrated uav-based mobility management," in *IEEE INFOCOM 2024 - IEEE Conference on Computer Communications Workshops (INFOCOM WKSHPS)*, 2024, pp. 1–8.
- [9] C. Adamczyk, "Challenges for conflict mitigation in o-ran's ran intelligent controllers," in *2023 International Conference on Software, Telecommunications and Computer Networks (SoftCOM)*. IEEE, 2023, pp. 1–6.
- [10] H. Zafar, E. Tohidi, M. Kasparick, B. Lorbeer, H. Lehmann, M. Weh, G. Rastogi, J. Charaf, M. Tarwala, A. Kliks *et al.*, "Ric-apps conflict management," i14y Lab, Tech. Rep., 2024.
- [11] M. Hoffmann, S. Janji, A. Samorzewski, L. Kułacz, C. Adamczyk, M. Dryjański, P. Kryszkiewicz, A. Kliks, and H. Bogucka, "Open ran xapps design and evaluation: Lessons learnt and identified challenges," *IEEE Journal on Selected Areas in Communications*, vol. 42, no. 2, pp. 473–486, 2024.
- [12] M. Polese, L. Bonati, S. D'Oro, S. Basagni, and T. Melodia, "Colo-ran: Developing machine learning-based xapps for open ran closed-loop control on programmable experimental platforms," *IEEE Transactions on Mobile Computing*, vol. 22, no. 10, pp. 5787–5800, 2023.
- [13] A. Lacava, M. Polese, R. Sivaraj, R. Soundararajan, B. S. Bhati, T. Singh, T. Zugno, F. Cuomo, and T. Melodia, "Programmable and customized intelligence for traffic steering in 5g networks using open ran architectures," *IEEE Transactions on Mobile Computing*, vol. 23, no. 4, pp. 2882–2897, 2024.
- [14] M. Huang and J. Chen, "Proactive mobility load balancing through interior-point policy optimization for open radio access networks," *IEEE Transactions on Mobile Computing*, vol. 24, no. 2, pp. 500–506, 2025.
- [15] J. Dai, L. Li, R. Safavinejad, S. Mahboob, H. Chen, V. V. Ratnam, H. Wang, J. Zhang, and L. Liu, "O-ran-enabled intelligent network slicing to meet service-level agreement (sla)," *IEEE Transactions on Mobile Computing*, vol. 24, no. 2, pp. 890–906, 2025.
- [16] H. Zhang, H. Zhou, and M. Erol-Kantarci, "Team learning-based resource allocation for open radio access network (o-ran)," in *ICC 2022 - IEEE International Conference on Communications*, 2022, pp. 4938–4943.
- [17] A. Wadud, F. Golpayegani, and N. Afraz, "Conflict management in the near-rt-ric of open ran: A game theoretic approach," in *2023 IEEE International Conferences on Internet of Things (iThings) and IEEE Green Computing & Communications (GreenCom) and IEEE Cyber, Physical & Social Computing (CPSCom) and IEEE Smart Data (SmartData) and IEEE Congress on Cybermatics (Cybermatics)*. IEEE, 2023, pp. 479–486.
- [18] A. Wadud, F. Golpayegani, and N. Afraz, "Qacm: Qos-aware xapp conflict mitigation in open ran," *IEEE Transactions on Green Communications and Networking*, vol. 8, no. 3, pp. 978–993, 2024.
- [19] H. Erdol, X. Wang, R. Piechocki, G. Oikonomou, and A. Parekh, "xapp distillation: Ai-based conflict mitigation in b5g o-ran," *arXiv preprint arXiv:2407.03068*, 2024.
- [20] P. B. del Prever, S. D'Oro, L. Bonati, M. Polese, M. Tsampazi, H. Lehmann, and T. Melodia, "Pacifista: Conflict evaluation and management in open ran," *arXiv preprint arXiv:2405.04395*, 2024.
- [21] A. Zolghadr, J. F. Santos, L. A. DaSilva, and J. Kibilda, "Learning and reconstructing conflicts in o-ran: A graph neural network approach," *arXiv preprint arXiv:2412.14119*, 2024.
- [22] J. Armstrong, E. Fallon, and S. Fallon, "Pre-emptive conflict detection architecture for o-ran service management and orchestration," in *2024 IEEE International Conference on Industry 4.0, Artificial Intelligence, and Communications Technology (IAICT)*, 2024, pp. 335–340.
- [23] A. Sultana, F. Bashar, M. R. Chowdhury, and A. P. Da Silva, "A software-defined radio based o-ran platform for xapp conflict detection and mitigation," in *MILCOM 2024 - 2024 IEEE Military Communications Conference (MILCOM)*, 2024, pp. 686–687.
- [24] T.-Y. Ross and G. Dollár, "Focal loss for dense object detection," in *proceedings of the IEEE conference on computer vision and pattern recognition*, 2017, pp. 2980–2988.
- [25] R. Aljundi, G. Farquhar, E. Ricci, S. Maskell, S. Shah, A. Javed, M. Besserve, T. Cohn, and M. Defferrard, "Graph u-nets," in *Proceedings of the 36th International Conference on Machine Learning (ICML)*, 2019.

Maryam Al Shami (Women in Engineering Member, IEEE) is a PhD can-

didate at Concordia Institute for Information Systems Engineering, Montreal, QC, Canada. Her current research focus is on proactive network management and root cause analysis in 5G RAN and beyond. Her research interests include 5G Networks and Beyond, Self-Healing Networks, Explainable AI/ML, Causal Discovery, Root Cause Analysis, and Predictive Maintenance.

**Jun Yan** (Member, IEEE) is the Concordia University Research Chair (Tier 2) in Artificial Intelligence in Cyber Security and Resilience and an Associate Professor at Concordia Institute for Information Systems Engineering, Montreal, QC, Canada. His research interests include cyber-physical systems and security, applied and adversarial computational intelligence, smart grids, smart transportation, smart cities, and attack-resilient systems and control.

**Emmanuel Thepie Fapi** is a Senior Data Scientist at Ericsson Canada, AI Hub Canada, Montreal. Prior to Ericsson, he worked as a Software Developer with Amazon Lab126, QNX Software System Limited, GENBAND U.S. LLC, MDA Systems, and Easy G. He holds a PhD from IMT Atlantique in signal processing and telecommunications in Brest, France. He also received a master's degree in engineering mathematics and computer tools from Orleans University in France. His research interests are 5G Networks and Beyond, Distributed AI/ML, Edge Computing, Autonomous Vehicles, Sustainable AI, Trustworthy AI, Non-Terrestrial Networks, Zero-Trust Architecture, Embedded Systems, and Advanced Digital Signal Processing.